The $^{11}\mathrm{B}(\vec{p},\gamma)^{12}\mathrm{C}$ reaction below 100 keV

J. H. Kelley,[1,2] R. S. Canon,[1,3] S. J. Gaff,[1,3] R. M. Prior,[1,4] B. J. Rice,[1,3] E. C. Schreiber,[1,3] M. Spraker,[1,4] D. R. Tilley,[1,2] E. A. Wulf,[1,3] and H. R. Weller[1,3]

[1]*Triangle Universities Nuclear Lab, Duke University, Durham, North Carolina 27708*

[2]*Department of Physics, North Carolina State University, Raleigh, North Carolina 27696*

[3]*Department of Physics, Duke University, Durham, North Carolina 27708*

[4]*Department of Physics, North Georgia College and State University, Dahlonega, Georgia 30597*

(Received 5 April 2000; published 6 July 2000)

The $^{11}\mathrm{B}(\vec{p},\gamma)^{12}\mathrm{C}$ reaction was studied by measuring the γ rays that were produced when 80–100-keV polarized protons were stopped in a thick $^{11}\mathrm{B}$ target. Cross sections and vector analyzing powers at 90° were determined as a function of energy for capture to the ground and first excited states of $^{12}\mathrm{C}$. These analyzing powers are particularly sensitive to the interference between *s*- and *p*-wave contributions, and to the relative phase between direct and resonance amplitudes. The results were used to produce a reliable extrapolation of the astrophysical *S* factor at 0 keV by means of a direct-capture-plus-resonances model calculation. The value of $S(0)$ that was obtained for $^{11}\mathrm{B}(p,\gamma_0)$, 1.8 ± 0.4 keV b, is in agreement with previously determined values, but for $^{11}\mathrm{B}(p,\gamma_1)$ the value of $S(0)$ is 3.5 ± 0.6 keV b and is more than twice as large as previously determined values.

PACS number(s): 25.40.Lw, 21.10.Pc, 24.70.+s, 27.20.+n

I. INTRODUCTION

The $^{11}\mathrm{B}(\vec{p},\gamma)^{12}\mathrm{C}$ reaction has been studied in an effort to better determine the low-energy reaction dynamics. Difficulties presented by low count rates, cosmic-ray backgrounds, and rapidly changing energy-dependent cross sections at very low beam energies complicate an accurate determination of absolute cross sections for this reaction. Therefore, the goal of this work is to measure spin-dependent observables with polarized protons, and to use these results to constrain a direct-capture-plus-resonances model and obtain a more reliable extrapolation of the astrophysical *S* factor for this reaction. Measurements of the energy-dependent reaction cross sections and vector analyzing powers (A_y) at 90° have been conducted at proton energies ranging from 80 to 100 keV.

The cross section for proton capture on $^{11}\mathrm{B}$ leading to $^{12}\mathrm{C}$ is small at astrophysically relevant energies ($E_p \leqslant 100$ keV) because of the large Coulomb barrier. In primordial nucleosynthesis, the less favorable proton capture reaction on $^{11}\mathrm{B}$ is often neglected, and $^{12}\mathrm{C}$ creation is assumed to proceed by neutron capture on $^{11}\mathrm{B}$ followed by the subsequent β decay of $^{12}\mathrm{B}$ into $^{12}\mathrm{C}$. In stellar nucleosynthesis, the $^{4}\mathrm{He}$ density, produced in the *p*-*p* chain, is large so that the triple-α reaction is responsible for generating most of the $^{12}\mathrm{C}$ nuclei. However proton capture on $^{11}\mathrm{B}$ cannot be entirely neglected.

Measurements of the low-energy $^{11}\mathrm{B}(p,\gamma)$ reaction rate have mainly focused on the narrow ~5-keV-wide capture resonance at $E_p = 163$ keV. Because of the low proton energy of this resonance and narrow width, level parameters for this state must be deduced from thick target yield measurements. A study of this resonance via $^{11}\mathrm{B}(p,\gamma_{0+1})$, by Anderson *et al.* [1], deduced a width and a peak cross section ($\Gamma = 6.7$ keV and $\sigma_\gamma = 125$ μb) that differ from the adopted values of Ajzenberg-Selove [2] ($\Gamma = 5.3$ keV and $\sigma_\gamma = 158$ μb) by more than 20%. More recently, Cecil *et al.* [3] deduced values of $\Gamma = 5.4$ keV and $\sigma_\gamma = 130$ μb, and found that this resonance plays a key role in determining the $^{11}\mathrm{B}(p,\gamma)$ reaction rates at very low energies.

Reaction rates at projectile energies below the Coulomb barrier decrease exponentially with decreasing beam energy, because rates are dominated by the probability for barrier penetration. Since beam energy changes of 10–20 keV can lead to orders of magnitude changes in the cross section in this energy regime, the astrophysical *S* factor simplifies the interpretation of reaction cross sections by removing the energy dependence which arises from the Coulomb barrier penetration. The reaction cross section is written in terms of $S(E)$, the astrophysical *S* factor, as

$$\sigma(E) = \frac{S(E)\exp(-2\pi\eta)}{E}, \tag{1}$$

where $2\pi\eta = 31.29 Z_{target} Z_{projectile}\sqrt{\mu/E}$, μ is the reduced mass in atomic mass units, and E is the center-of-mass energy in keV.

The *S* factor could be expected to have a simple energy dependence, if only the Coulomb barrier influenced the reaction rates. However, capture strength from near-threshold resonances can lead to rapidly varying reaction cross sections, and their influence on the *S* factor must be fully considered. Relatively small non-*s*-wave contributions from near-threshold resonances are measurable due to the fact that their interference with the usually dominant *s*-wave amplitude can be observed in asymmetric cross-section angular distributions and in nonzero vector analyzing powers at $\theta = 90°$. The analyzing power at $\theta = 90°$, $A_y(90°)$, is finite only if multipoles of opposite parity are present. The quantities that we measured, including $A_y(90°)$, are used to constrain a direct-capture-plus-resonances model in an attempt to better predict the capture rate at astrophysically relevant energies, at a few tens of keV.

Previous studies of polarized proton $\vec{p}$ capture on ^{7}Li [4,5] and ^{9}Be [6], at proton energies of 100 keV and below, have found evidence for non-*s*-wave contributions in the capture strength. In the case of $^7\mathrm{Li}(p,\gamma)$, for example, significant *p*-wave strength from the resonance tail of a subthreshold state leads to a factor of 2 increase over the *S* factor deduced without this resonance [5]. The discovery of *p*-wave strength in proton capture on ^{7}Li and ^{9}Be [4–6] challenges the common assumption that, at very low energies, only *s* waves contribute significantly to capture because of sizable angular momentum barriers.

II. EXPERIMENTAL DETAILS

In the present measurements, we detected the γ rays that were emitted when a 30–50-μA beam of polarized protons from the Atomic Beam Polarized Ion Source (ABPIS) at the Triangle Universities Nuclear Laboratory impinged on a thick ^{11}B target. The proton beams were 70–85 % polarized in the spin-up–spin-down directions, and a fast spin-flip controller was used to reverse the proton polarization axis at a rate of 10 Hz.

The target was produced by electron-gun evaporation of 98.5% pure samples of ^{11}B onto a Ta foil backing. The evaporated ^{11}B layer was 260 μg/cm^2 thick, and was sufficient to stop the proton beam. Therefore, γ rays were produced for the entire range from $E_p = E_{incident}$ to $E_p = 0$. Due to the rapidly decreasing cross section, ~85% of the detected γ rays were produced in the first 15 keV of energy loss.

To obtain measurements at proton energies higher than 80 keV, the maximum energy that the ABPIS can deliver, a computer controlled negative high-voltage power supply was attached to the target, and was used to increase the energy of the H^+ beam. However, because it was not possible to measure the beam current while strongly biasing the target, the beam intensity, and target stability were monitored by measuring the α particles (α_0 and α_1) that were produced in $^{11}\mathrm{B}(p,\alpha)$ reactions. These reactions have a much higher cross section (a factor ≈ 500 for α_0) than the (p,γ) reaction and have essentially no background for the α_0-particle reaction products. Therefore, using the cross section data of Angulo *et al.* [7], the $^{11}\mathrm{B}(p,\alpha_0)$ count rate provided a reliable means to measure the beam current and to monitor the target condition.

We were able to accelerate the H^+ ions by as much as 20 keV using the negative high-voltage supply. This permitted measurements of the energy-dependent reaction cross sections at energies from 80 to 100 keV. The energy dependence of the cross section was obtained from a systematic measurement of the relative γ-ray flux for runs with different beam energies (target biases). In an attempt to average out possible beam fluctuations, data collection was grouped into relatively short cycles of runs. During a cycle, data were taken at all sampled energies, and it was assumed that the beam and target characteristics did not change appreciably. For example, a cycle of relatively short runs with proton energies ranging from 80 to 100 keV, with 10-keV steps, were carried out in a matter of 70 min. This relatively short period was divided to give approximately equal yield for γ rays at the sampled energies. At the completion of a cycle the process was repeated.

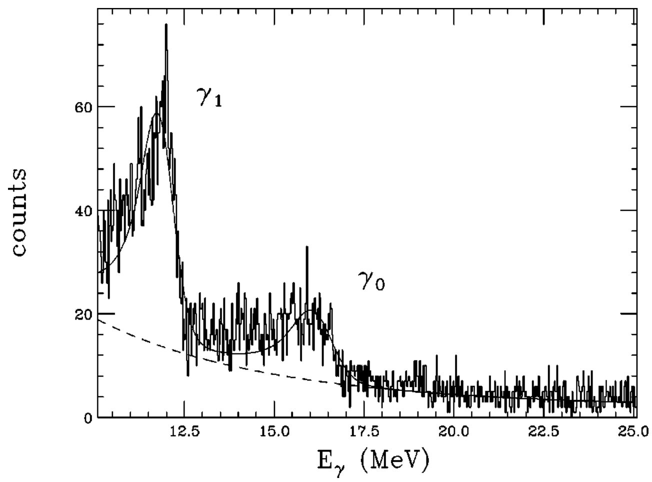

FIG. 1. A typical γ-ray spectrum showing γ_0 and γ_1 obtained at $\theta = 90°$ and $E_{inc} = 100$ keV. The γ-ray capture lines are discussed in the text.

A 25-cm diameter by 25-cm long NaI detector was used to detect the γ rays ($\gamma_0 \approx 16$ MeV and $\gamma_1 \approx 12$ MeV) with 3–5 % energy resolution. A 4-in.-thick plastic annulus acted as an anticoincidence shield to reject cosmic-ray events. The anticoincidence shield provided over 98% cosmic-ray rejection, and greatly minimized the background. A typical γ-ray spectrum, obtained at $E_{inc} = 100$ keV using the anticoincidence shield, is shown in Fig 1. The dashed curve shows the cosmic-ray background that was measured during a beam-off run, and normalized in the region above 19 MeV. The solid curve in the figure shows the response function of the NaI detector, measured in the $^3\mathrm{H}(p,\gamma)$ reaction, fit to the γ_0 and γ_1 capture lines.

The γ-ray flux was extracted from the measured spectra following a background subtraction. The response function of the detector has been measured and yields an efficiency of 57% for detecting γ rays in a region that is approximately one width above the γ-ray peak energy and two widths below the peak energy [8]. The background, which was primarily from cosmic rays, was measured during ''beam-off'' runs, and was fit with a polynomial function. The background was subtracted from the beam-on spectra following a normalization in the region above 19 MeV.

Because the γ rays and α particles are produced at proton energies from $E_p = E_{inc}$ to $E_p = 0$, the energy-dependent cross sections were obtained using a convolution integral that included a parametrized *S* factor and the proton stopping powers. As in Cecil *et al.* [3] the γ-ray cross section is determined from a comparison of the γ-ray to charged-particle (α_0) ratio using the expression

$$\frac{Y_\gamma(E_{inc})}{Y_\alpha(E_{inc})} = \frac{\mathrm{eff}_\gamma(E_\gamma)}{\mathrm{eff}_\alpha(E_\alpha)} \times \frac{\int \sigma_\gamma(E_p) f(E_p)/\epsilon(E_p)\, dE_p}{\int \sigma_\alpha(E_p) f(E_p)/\epsilon(E_p)\, dE_p}. \quad (2)$$

TABLE I. Measured reaction cross sections and analyzing powers at 90°.

E_{beam} (keV)	A_y 90° γ_0	Measured $\sigma(\gamma_0)$ (nb)	A_y 90° γ_1	Measured $\sigma(\gamma_1)$ (nb)
80	−0.12(0.18)	0.94(0.18)	0.29(0.11)	2.17(0.41)
90	+0.14(0.12)	2.41(0.47)	0.45(0.07)	6.42(1.16)
100	+0.06(0.07)	5.14(0.94)	0.40(0.07)	15.8(2.7)

Y is the yield of γ rays or α particles that were produced as the protons were stopped in the target ($E_p = E_{inc}$ to $E_p = 0$), the eff(E)'s represent the detector efficiencies, the $\sigma(E_p)$'s are the energy-dependent cross sections, and $f(E_p)$ and $\epsilon(E_p)$ are the atomic fraction of target nuclei and the stopping power in the target for E_p, respectively.

The stopping powers that were used in the convolution integral were from Anderson and Ziegler [9], the cross sections for $^{11}B(p,\alpha_0)$ were from the evaluation of Rauscher and Raimann [10] and the cross sections for γ_0 and γ_1 used parametrized S factors that had the forms of a constant term plus a Breit-Wigner contribution for the resonance at $E_p = 163$ keV. The cross sections of the present work were obtained by fixing the Breit-Wigner terms of the parametrized S factors to reproduce the $E_p = 163$ keV resonance peak cross sections deduced by Cecil *et al.* [3], and adjusting the constant terms to reproduce the γ-ray yields observed in our measurement. The cross sections and S factors presented below correspond to the values of the parametrized S factors at $E_p = E_{inc}$. Alternatively, we fixed the constant terms in the S factors, and adjusted the strength of the Breit-Wigner terms to reproduce our observed γ-ray yields. The small differences in the cross sections deduced by these two methods are about 4–8 %. Finally, the shapes of the S factors deduced from our direct-capture-plus-resonances model, discussed below, were used in the convolution integral with a normalization factor, and the cross sections deduced with this method agreed with the results of the former method, described above, within 5%.

III. RESULTS

We measured the energy dependence of both the cross section and the analyzing power at 90° for $^{11}B(p,\gamma)^{12}C$ at $E_{inc} = 80$–100 keV. The results are presented in Table I. The method described above to obtain S factors and cross sections yields values that correspond to $E_p = E_{inc}$; however, because the experiment uses thick targets the analyzing powers correspond to the values at an ''effective'' energy which is ~ 6 keV below the incident proton energy. The systematic uncertainties for determining absolute reaction cross sections, discussed below, lead us to place most emphasis on the analyzing powers and S factor slopes (relative cross sections) since these observables are not strongly affected by systematic effects.

A determination of absolute cross sections from our data is complicated by the fact that the target bias of up to 20 kV prevented a direct measurement of the beam current. Also, the large 25-cm-diameter detector was placed very close to the target (≈ 22.5 cm from the target to the front face of the detector), so that finite geometry corrections were substantial. In addition, measurements of low-energy reaction cross sections are sensitive to impurities in the target which result from oxidation or other processes that affect the composition of the target. Previous studies using boron targets, for example by Anderson *et al.* [1] and Angulo *et al.* [7], found significant oxidation. Although we did not rigorously study the composition of our targets, the γ-ray to α-particle ratio should be relatively insensitive to the effects of small target impurities. For these reasons, we place most emphasis on the analyzing powers and S factor slopes. The statistical uncertainties in our data are about 5–10 %, while uncertainties in the detector efficiencies and solid angles are about 10%, and the uncertainties in the convolution integrals are taken as 10%. The $E_p = 100$ keV S factors that we measured are $S_{\gamma 0} = 3.09 \pm 0.56$ keV b for $^{11}B(p,\gamma_0)$ and $S_{\gamma 1} = 9.49 \pm 1.65$ keV b for $^{11}B(p,\gamma_1)$; these values are in agreement with the values that were previously determined by the parametrization of Cecil *et al.* [3] ($S_{\gamma 0} = 2.29 \pm 0.46$ keV b and $S_{\gamma 1} = 8.79 \pm 1.32$ keV b for $E_p = 100$ keV).

IV. ANALYSIS AND CALCULATIONS

The measurement of analyzing powers and S factor slopes at low energies, in combination with higher-energy cross-section data, usually collected with much higher statistics, can provide sufficient constraints so that a reliable extrapolation of the value of the S factor at $E_p = 0$ can be performed. Fig. 2 shows the high-energy data of Segel *et al.* [11] and Allas *et al.* [12] (500 keV and above), compared with a direct-capture calculation that is based on the spectroscopic factors from Cohen and Kurath [13]. Low-energy resonances at 163 keV, 675 keV, and 1.4 MeV are seen to dominate the cross section, while the giant dipole resonance is seen at higher energies. These correspond to ^{12}C states at $16.10(2^+)$, $16.57(2^-)$, $17.23(1^-)$, $22.6(1^-)$, and $25.4(1^-)$ MeV, respectively.

We used the data of Segel *et al.* [11], the spectroscopic factors from Cohen and Kurath [13], and the resonance parameters from Ajzenberg-Selove [2] to determine the strengths of the resonances in our direct-capture-plus-resonances calculation. Extrapolations of the S factor to zero energy based solely on reaction cross-section data can be ambiguous because solutions with different relative phases for the resonance interference terms can be found which reasonably reproduce the existing data while predicting significantly different results at $E_p = 0$. Our analyzing powers and S factor slopes provide additional constraints on the calculations, thus permitting a more reliable extrapolation of the astrophysical S factor into the as yet unmeasured but astrophysically important energy region below $E_p = 50$ keV.

A. Direct-capture-plus-resonances model

Our model uses a direct semidirect formalism [14] to include interference effects between direct-capture and reso-

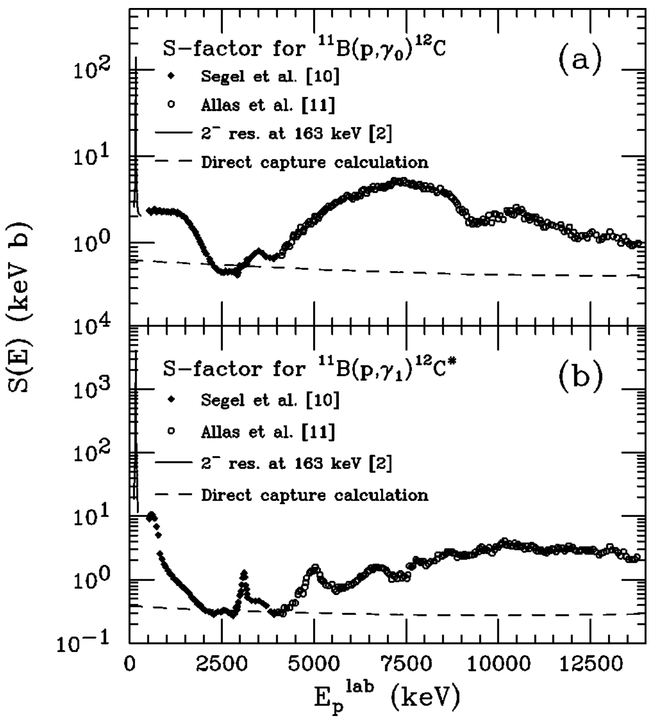

FIG. 2. Previously reported cross-section data plotted as astrophysical S factors for the $^{11}\mathrm{B}(\vec{p},\gamma_0)$ (a) and $^{11}\mathrm{B}(\vec{p},\gamma_1)$ (b) reactions at higher energies [11,12] compared with a calculation (dashed line) of the direct-capture contributions.

nance strengths. The direct-capture amplitude and the resonant (semidirect) amplitude radial matrix elements are combined as

$$\langle u(r)|r|\chi^+(r)\rangle+\sum_{i=1}^{n}\left\langle u(r)\left|\frac{g(r)_i}{E-E_{Ri}+i\Gamma_i/2}\right|\chi^+(r)\right\rangle. \tag{3}$$

The single-particle bound-state wave functions $u(r)$ were generated from Woods-Saxon potentials ($r=1.25$ and $a=0.65$) whose depths were adjusted to reproduce the experimental values of the binding energies. This same potential was used to generate the scattering wave function $\chi^+(r)$. The ''resonance strengths'' $g(r)_i$ are based on derivative Woods-Saxon shapes whose magnitudes were adjusted to fit the on-resonance cross sections, while the signs of $g(r)_i$ determine an overall relative phase between the various direct and resonance amplitudes.

Our aim is to perform a simple calculation that takes into account the influence of near-threshold resonances, and describes the low-energy behavior of the cross section. In order to simplify the calculation we limited the model to $E1$ direct capture and the three lowest resonances (the $E2$, $E3$, and $M1$ direct-capture strengths were found to have a negligible influence on the calculated cross sections and analyzing powers, and have therefore been omitted), although interference with the tails of the giant dipole resonance may influence the low-energy reaction cross sections. Our model uses the single-level approximation, and is not appropriate for treating the interference of states with identical J^π; we as-

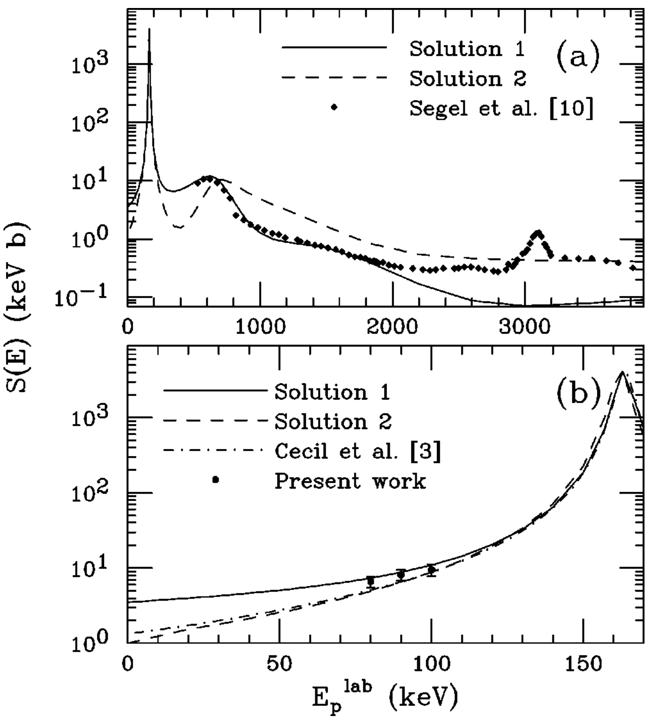

FIG. 3. The reaction cross-section data for the $^{11}\mathrm{B}(p,\gamma_1)$ reaction, shown as S factors, compared with predictions from a direct-capture-plus-resonances calculation. The solid and dashed curves indicate the sensitivity of the calculation to the details of the interference effects (see Table II). The dot-dashed curve of Fig. 3(b) was obtained using the S factor parametrization of Cecil *et al.* [3].

sumed that the low-lying 1^- resonance at $E_p=1.4$ MeV was dominant in our energy regime.

B. First-excited-state capture γ_1 rays

Capture to the first excited state has a cross section that is considerably larger than capture to the ground state at the energies we studied. Therefore, because of the low statistics obtained, we have focused most of our attention on capture to the first excited state. Our calculations for capture to the 4.4-MeV state of ^{12}C include $E1$ direct-capture amplitudes and resonances at 16.10 (2^+), 16.57 (2^-), and 17.23 (1^-) MeV. Because of uncertainties in the precise values of the width and peak cross section for the $E_p=163$ keV resonance, the strength of this resonance was adjusted to reproduce the peak cross section measured by Cecil *et al.* [3].

The relative phases (signs) of the resonance amplitudes [see Eq. (3)] determine whether the interference contributions are constructive or destructive, and the importance of these interference effects is seen in Fig. 3. The solid and dashed curves of Fig. 3 represent different predictions that are obtained by changing the relative phases of the resonance amplitudes as detailed in Table II; the different values of the S factor at $E_p=0$ show the sensitivity to this interference. The $^{11}\mathrm{B}(p,\gamma_1)$ resonance parameters used in this calculation are given in Table II.

Our measurement of the relative cross sections (S factor slope) is not, by itself, adequate to determine which solution

TABLE II. Resonance parameters for capture to the ^{12}C first excited state γ_1.

$E_{resonance}$ (keV)	$\Gamma_{(c.m.)}$ (keV)	Solution I strength (keV^2/fm^2)	Solution II strength (keV^2/fm^2)
163 keV	5.3 keV	−399.3	−409.2
675 keV	300 keV	−82.5	+90.0
1388 keV	1150 keV	−80.0	−65.0

is the physically correct one, as can be seen in Fig. 3(b). Fortunately, the analyzing powers can be used to select the "correct" solution. Figure 4 displays a plot of the predictions of the value of $A_y(90°)$ for the two solutions, along with the measured values. The analyzing powers are sensitive to the *s*- and *p*-wave interference effects of the reaction, while having little sensitivity to most experimental effects that complicate absolute cross-section measurements.

The measured $^{11}B(\vec{p},\gamma_1)$ analyzing powers are in best agreement with the solid line in Fig. 4, which corresponds to a value of $S(0)=3.5\pm0.6$ keV b; the uncertainty is obtained from the uncertainty in the measurement at $E_{inc}=100$ keV, and does not include any systematic error associated with the extrapolation procedure. This extrapolation is significantly larger ($\approx$2.5 times) than that obtained by Cecil *et al.* [3]: $S(0)=1.3\pm0.3$ keV b.

C. Ground-state capture γ_0 rays

The poor statistics of our measurement limit our comment in regard to the $^{11}B(p,\gamma_0)$ reaction, and although our measurements are in agreement with the measurements of Cecil *et al.* [3], within the uncertainties, our values are systematically larger [see Fig. 5(b)]. We have performed calculations

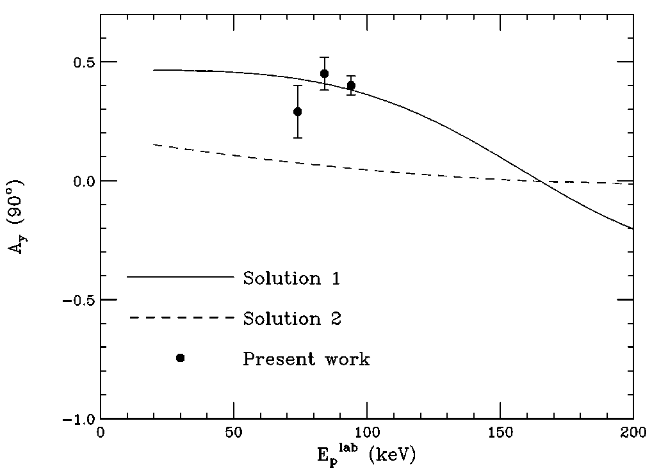

FIG. 4. The analyzing powers measured at 90° for the $^{11}B(\vec{p},\gamma_1)$ reaction compared with predictions from a direct-capture-plus-resonances calculation. In the figure the data are given in terms of $E_p=E_{effective}$, which is ~6 keV below E_{inc}. The solid and dashed curves indicate the sensitivity of the calculation to the details of the interference effects (see Table II).

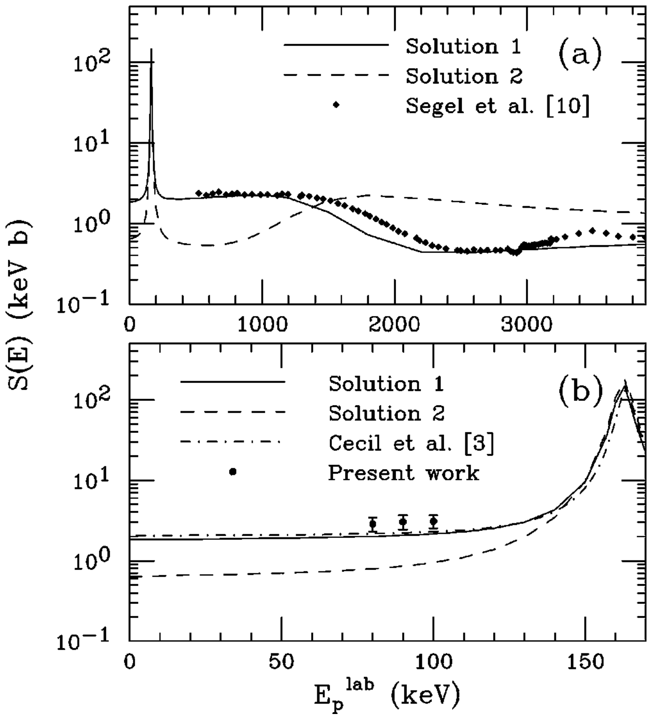

FIG. 5. Predictions of the *S* factor of the $^{11}B(p,\gamma_0)$ reaction. The solid and dashed curves in (a) show the sensitivity of the calculations to interference effects (see Table III). The dot-dashed curve of (b) was obtained using the *S* factor parametrization of Cecil *et al.* [3].

for capture to the ground state of ^{12}C that include only $E1$ direct capture and the two resonant states at 16.1 MeV (2^+) and 17.23 MeV (1^-). As above, the solid and short dashed curves in Fig. 5 indicate the sensitivity of the reaction to the details of the interference effects. Changing the relative phases of the resonance amplitudes leads to significantly different values of the *S* factor at $E_p=0$. The $^{11}B(p,\gamma_0)$ resonance parameters used in this calculation are given in Table III.

The solid curve yields $S(0)=1.8\pm0.4$ keV b, and is in agreement with the measured values of Cecil *et al.* [3] and their extrapolation to lower energies, which gives $S(0)=2.0\pm0.4$ keV b. The solid curve yields a rather poor fit to the data of Segel *et al.* [11] above 1 MeV, which may indicate contributions from the giant dipole resonance at 22.6 MeV (1^-) and 25.4 MeV (1^-). The dashed curve is clearly not in agreement with either the data of Segel *et al.* [11] or the present results. For reasons stated above, our model is

TABLE III. Resonance parameters for capture to the ^{12}C ground state γ_0.

$E_{resonance}$ (keV)	$\Gamma_{(c.m.)}$ (keV)	Solution I strength (keV^2/fm^2)	Solution II strength (keV^2/fm^2)
163 keV	5.3 keV	−729.1	−729.1
1388 keV	1150 keV	−60.0	+60.0

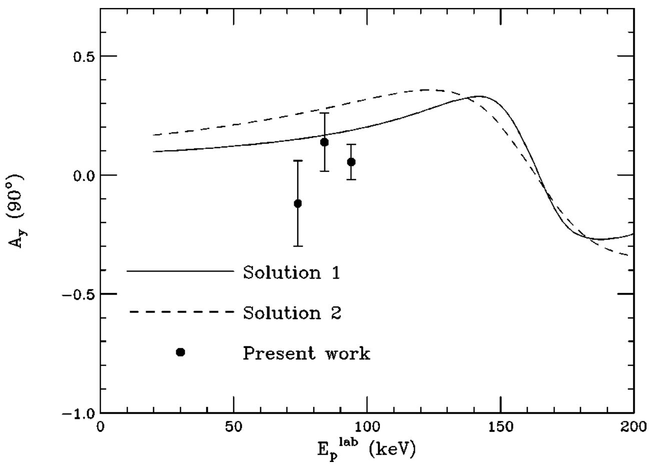

FIG. 6. The analyzing powers measured at 90° for the $^{11}B(\vec{p},\gamma_0)$ reaction compared with predictions from a direct-capture-plus-resonances calculation. In the figure the data are given in terms of $E_p = E_{effective}$, which is ~6 keV below E_{inc}. The solid and dashed curves indicate the sensitivity of the calculation to the details of the interference effects (see Table III).

unable to produce a reliable prediction in regions where multiple 1^- states contribute. In addition, because of low statistics, the fit to the analyzing power data, shown in Fig. 6, is somewhat inconclusive.

V. CONCLUSIONS

We have measured the energy-dependent reaction cross sections and analyzing powers for the $^{11}B(\vec{p},\gamma)$ reaction between 80 and 100 keV. Nonzero vector-analyzing powers were found at 90°, indicating *s*- and *p*-wave interference in proton capture on ^{11}B at energies below 100 keV. Using these measurements and previously measured higher-energy reaction cross-section data as constraints, we made detailed calculations that include interference effects between the direct-capture strength and the participating resonances. These calculations give insight into the low energy reaction dynamics, and emphasize the importance of interference effects. The value of $S(0)$ that we obtain for the $^{11}B(p,\gamma_0)$ reaction, 1.8 ± 0.4 keV b, is in agreement with previous measurements. However the value for the $^{11}B(p,\gamma_1)^{12}C^*$ reaction, $S(0) = 3.5 \pm 0.6$ keV b, is considerably larger than earlier extrapolations. This illustrates that the influence of low-lying resonances is important for determining low-energy reaction rates, and that polarization data are essential in order to understand the effects of these resonances in any attempt to extrapolate measured cross sections to astrophysically relevant energies.

ACKNOWLEDGMENTS

This work was partially supported by the Department of Energy under Grant Nos. DE-FG02-97ER41033, DE-FG02-97ER41042, and DE-FG02-97ER41046.

[1] B.D. Anderson, M.R. Dwarakanath, J.S. Schweitzer, and A.V. Nero, Nucl. Phys. **A233**, 286 (1974).
[2] F. Ajzenberg-Selove, Nucl. Phys. **A506**, 1 (1990).
[3] F.E. Cecil, D. Ferg, H. Liu, J.C. Scorby, J.A. McNeil, and P.D. Kunz, Nucl. Phys. **A539**, 75 (1992).
[4] M.A. Godwin, R.M. Chastler, C.M. Laymon, R.M. Prior, D.R. Tilley, and H.R. Weller, Phys. Rev. C **53**, R1 (1996).
[5] M. Spraker, R.M. Prior, M.A. Godwin, B.J. Rice, E.A. Wulf, J.H. Kelley, D.R. Tilley, and H.R. Weller, Phys. Rev. C **61**, 015802 (2000).
[6] E.A. Wulf, M.A. Godwin, J.F. Guillemette, C.M. Laymon, R.M. Prior, B.J. Rice, M. Spraker, D.R. Tilley, and H.R. Weller, Phys. Rev. C **58**, 517 (1998).
[7] C. Angulo, S. Engstler, G. Raimann, C. Rolfs, W.H. Schulte, and E. Somorjai, Z. Phys. A **345**, 231 (1993).
[8] H.R. Weller and N.R. Roberson, IEEE Trans. Nucl. Sci. **28**, 1268 (1981); Evans Haywood (private communication).
[9] H.H. Anderson and J.F. Ziegler, *Hydrogen Stopping Powers and Ranges in all Elements* (Pergamon, New York, 1977).
[10] T. Rauscher and G. Raimann, Phys. Rev. C **53**, 2496 (1996).
[11] R.E. Segel, S.S. Hanna, and R.G. Allas, Phys. Rev. **139**, B818 (1965).
[12] R.G. Allas, S.S. Hanna, Luis Meyer-Schützmeister, and R.E. Segel, Nucl. Phys. **58**, 122 (1964).
[13] S. Cohen and D. Kurath, Nucl. Phys. **A101**, 1 (1967).
[14] H.R. Weller and N.R. Roberson, Rev. Mod. Phys. **52**, 699 (1980).